Contract No:

This document was prepared in conjunction with work accomplished under Contract No. DE-AC09-08SR22470 with the U.S. Department of Energy (DOE) Office of Environmental Management (EM).

Disclaimer:

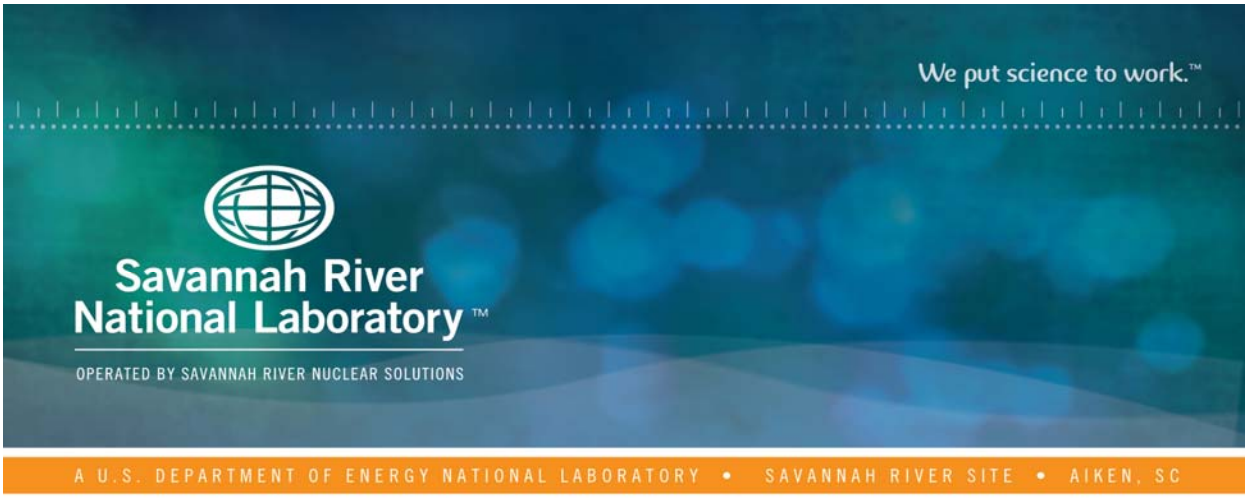

Optimized Dissolution Flowsheet for Uranium Metal

W. E. Daniel

T. S. Rudisill

June 2018

SRNL-STI-2018-00180, Revision 0

DISCLAIMER

Printed in the United States of America

Prepared for
U.S. Department of Energy

SRNL-STI-2018-00180
Revision 0

Keywords: *Uranium Metal, Dissolution, Molybdenum-99, General Atomics*

Retention: *Permanent*

Optimized Dissolution Flowsheet for Uranium Metal

W. E. Daniel
T. S. Rudisill

June 2018

Prepared for the U.S. Department of Energy under contract number DE-AC09-08SR22470.

Savannah River National Laboratory™
OPERATED BY SAVANNAH RIVER NUCLEAR SOLUTIONS

REVIEWS AND APPROVALS

AUTHORS:

_____
W. E. Daniel, Separations and Actinide Science Programs Date

_____
T. S. Rudisill, Separations and Actinide Science Programs Date

TECHNICAL REVIEW:

_____
P. M. Almond, Separations and Actinide Science Programs Date

APPROVAL:

_____
T. B. Brown, Manager Date
Separations and Actinide Science Programs

_____
D. E. Dooley, Director Date
Chemical Processing Technologies

PREFACE OR ACKNOWLEDGEMENTS

The authors would like to acknowledge the support of the SRNL Glass Shop for constructing and helping design the glassware used for the dissolution experiments. The Glass Shop was able to modify equipment designs and refabricate needed glassware within a matter of days which allowed the project to proceed on schedule.

EXECUTIVE SUMMARY

The U.S. Department of Energy's National Nuclear Security Administration (NNSA) has entered into cooperative agreements with commercial businesses to establish a reliable domestic source of ^{99}Mo that will be produced without the use of highly enriched uranium (HEU). NNSA's support of these businesses is based on a (50%/50%) government/commercial cost-share basis, with NNSA contributions up to a total of $25 million for each project. Molybdenum-99 is the parent isotope of ^{99m}Tc, the most widely used radioisotope in nuclear medical diagnostic imaging. It is employed in about 14 million procedures per year.[1] The United States does not currently produce ^{99}Mo and therefore imports all of its supply from foreign producers, some of which still use HEU in the production process.

In addition to the financial support provided directly to the commercial businesses, NNSA has also funded national laboratory support to assist in the commercialization of the ^{99}Mo production processes. The Savannah River National Laboratory (SRNL) is providing technical support to a cooperative agreement team which consists of General Atomics, the University of Missouri Research Reactor (MURR®), and Nordion. A single-use low enriched U target is under development by the General Atomics team to produce ^{99}Mo. The UO_2 targets will be irradiated at MURR® and transferred to a hot cell for ^{99}Mo recovery. The UO_2 targets will be fabricated by a private company using U metal enriched to 19.75% ^{235}U. To prepare the UO_2, the U metal must be initially dissolved to produce a uranyl nitrate ($UO_2(NO_3)_2$) solution. The dissolution rate of the metal using the current process is slow and is not considered acceptable for a production process. To address this issue, SRNL was requested to develop an optimized U metal dissolution process with an increased dissolution rate.

To develop the information necessary to specify an optimized flowsheet for the dissolution of U metal, laboratory experiments were performed to measure the effects of HNO_3 concentration, temperature, and the catalytic effects of fluoride and nitric oxide (NO) gas on the rate of dissolution. Uranium metal dissolutions with increasing HNO_3 concentration demonstrated that the dissolution rate was a strong function of the acid concentration consistent with data in the literature. The rate of dissolution increased by a factor of 12 between 4 and 10 M HNO_3. The optimum HNO_3 concentration for a U metal dissolution process depends upon the desired cycle time and the acid concentration required for downstream processing. The dissolution rate of U metal is not a strong function of temperature relative to acid strength. An increase in temperature from 90 to 110 ˚C during dissolutions performed in 8 M HNO_3 only resulted in a doubling of the rate. However, unless there is a reason to use a temperature less than the boiling point of the solution (e.g., safety concerns), performing U metal dissolutions at the boiling point is recommended to maximize the dissolution rate.

For the addition of fluoride to have a significant effect on the U metal dissolution rate, concentrations greater than 0.01 M were required. There was not a significant change in the dissolution rate in experiments performed with 0.01 M and no fluoride present in the solution. When 0.05 and 0.10 M fluoride were added to the solution, the measured rates increased by factors of approximately two and eight, respectively. The ineffectiveness of 0.01 M fluoride in catalyzing the U metal dissolution is likely due to the complexation of the fluoride by the U in solution. The use of fluoride to catalyze U metal dissolution must be balanced against the potential for corrosion of downstream equipment and the addition of corrosion product impurities to the U stream.

The laboratory experiments demonstrated that the use of NO gas is a viable option to accelerate the dissolution rate of U metal and is recommended for applications where high purity $UO_2(NO_3)_2$ is required. The NO sparge should saturate the dissolving solution and should not impinge directly upon the U metal which would result in a mass transfer limitation which interferes with HNO_3/HNO_2 reactions at the surface of the metal negatively impacting the dissolution rate.

TABLE OF CONTENTS

LIST OF TABLES

LIST OF FIGURES

LIST OF ABBREVIATIONS

ADU	ammonium diuranate
EBR-II	Experimental Breeder Reactor-II
INL	Idaho National Laboratory
HEU	highly enriched uranium
LEU	low enriched uranium
MURR®	University of Missouri Research Reactor
NNSA	National Nuclear Security Administration
SRNL	Savannah River National Laboratory

1.0 Introduction

1.1 Background

The U.S. Department of Energy's National Nuclear Security Administration (NNSA) has entered into cooperative agreements with commercial businesses to establish a reliable domestic source of ^{99}Mo that will be produced without the use of highly enriched uranium (HEU). NNSA's support to these businesses is based on a (50%/50%) government/commercial cost-share basis, with NNSA contributions up to a total of $25 million for each project. Molybdenum-99 is the parent isotope of ^{99m}Tc, the most widely used radioisotope in nuclear medical diagnostic imaging. It is employed in about 14 million procedures per year.[1] The United States does not currently produce ^{99}Mo and therefore imports all of its supply from foreign producers, some of which still use HEU in the production process.

In addition to the financial support provided directly to the commercial businesses, NNSA has also funded national laboratory support to assist in the commercialization of the ^{99}Mo production processes. The Savannah River National Laboratory (SRNL) is providing support to a cooperative agreement team which consists of General Atomics, the University of Missouri Research Reactor (MURR®), and Nordion. A single-use target is under development by the General Atomics team to produce ^{99}Mo. The UO_2 targets will be irradiated at MURR® and transferred to a hot cell for ^{99}Mo recovery. The UO_2 targets will be fabricated by a private company using U metal enriched to 19.75% ^{235}U. To prepare the UO_2, the U metal must be initially dissolved to produce a uranyl nitrate ($UO_2(NO_3)_2$) solution. The dissolution rate of the metal using the current process is slow and is not acceptable for a production process. To address this issue, SRNL was requested to develop an improved U metal dissolution process with an optimized dissolution rate.

1.2 Uranium Metal Dissolution

Uranium metal dissolution chemistry in HNO_3 is complicated, as the acid reduction products change as a function of the HNO_3 concentration. In general, dissolutions performed at HNO_3 concentrations less than or equal to 8 M produce primarily nitric oxide (NO) gas. Dissolutions performed at acidities greater than 8 M mostly result in the production of nitrogen dioxide (NO_2) gas.[2] There are many factors which may influence the dissolution rate of large pieces of U metal.[3] Factors inherent to the material itself which affect the dissolution rate include: impurities, metal treatment, grain size, shape, and surface area. Factors which can be manipulated during dissolution include: the HNO_3 concentration, temperature, use of a catalyst, and factors which influence the concentration of reaction products.

In a study which evaluated the presence of impurities in U metal, Lacher et al.[3] found that the presence of C and N was positively correlated with the ease of dissolution. The presence of large amounts of these elements resulted in a significant increase in the dissolution rate. Since these impurities were present in small quantities with respect to the amount of U, their effect upon the dissolution rate was assumed to be catalytic. In other studies, samples of U from lots of material which had been worked also tended to dissolve more rapidly along the direction of the axis from which they were cut; although, the presence of a small amount of impurities was required to observe this effect. Since the grain size of U metal decreased as the amount of work increased, the effect of metallurgical treatment on dissolution rate was attributed to the size and orientation of the metal grains. The anisotropic dissolution of U metal which has been worked also caused the shape of the metal sample to be a factor influencing the dissolution rate. The mass of U metal dissolved as a function of time is clearly proportional to the total surface area. An apparent increase or decrease in the dissolution rate of U metal as the reaction proceeds may in part be attributed to a change in total surface area.

Variables which are easily changed during U metal dissolution include the HNO_3 concentration and the solution temperature. The dissolution rate is strongly dependent on the HNO_3 concentration. Lacher et al.[3]

performed dissolutions at 0 and 25 ˚C and observed the behavior plotted on Figure 1-1. The maximum rates were obtained in 13 to 14 M HNO_3. At higher concentrations, the rate decreased which likely can be attributed to passivation of the metal surface by the highly oxidizing solution.

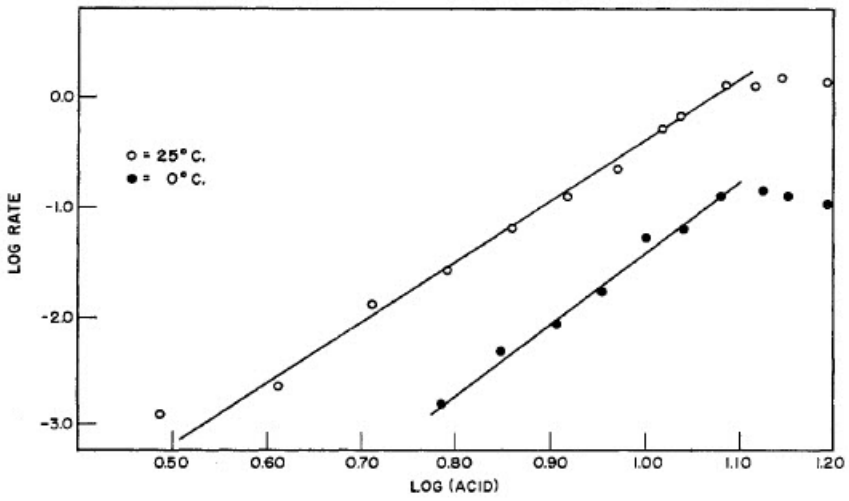

Figure 1-1. Dissolution Rate of U Metal in HNO_3 Solutions

The dissolution rate of U metal also increases with increasing metal concentration, which indicates a dependence on the total nitrate concentration.[4,5,6] Large scale dissolution processes for (depleted or natural) U metal (i.e., tons per day) take advantage of this property by maintaining a significant heel of U in the dissolver to maximize the concentration during the initial stages of a dissolution cycle. A heel is defined as metal remaining in a dissolver from a previous incomplete batch dissolution. Instantaneous dissolution rates have been measured for unirradiated ingots of U as a function of the total nitrate concentration. The data show that the dissolution rate at the boiling point of the solution is proportional to the cubed power of the total nitrate concentration. At a given total nitrate concentration, the dissolution rate is independent of the HNO_3 concentration or the U concentration.[5] For U dissolutions in which the concentration is controlled to a relatively low value, the effect of the metal concentration on the rate is relatively insignificant.

The dissolution rate of U metal also increases with increasing temperature. Lacher et al.[3] performed a series of dissolutions in 8.1 and 15.6 M HNO_3 using solution temperatures of 0, 25, and 50 ˚C. Figure 1-2 shows plots of the natural log of the initial rate versus the reciprocal of the absolute temperature. From the slopes of the lines through the data, the authors calculated activation energies of 15.9 and 12.2 kcal/mol for the dissolution of U metal in 15.6 and 8.1 M HNO_3, respectively.

The dissolution rate of U metal can be increased significantly by the addition of nitrite to the HNO_3 solution.[3,7] Lacher et al.[3] measured the instantaneous dissolution rate of U metal in a series of experiments using 6.0 and 15.6 M HNO_3 with the addition of varying concentration of potassium nitrite (KNO_2). The data (Figure 1-3) showed a significant dependence on the nitrite concentration. Since HNO_2 acid is in equilibrium with the gas reaction products (i.e., NO and NO_2) produced during U metal dissolution (equations 1 and 2),[8] it follows that the reaction is autocatalytic.

$$2NO_2 + H_2O \rightleftharpoons HNO_3 + HNO_2 \quad (1)$$

$$NO + NO_2 + H_2O \rightleftharpoons 2HNO_2 \quad (2)$$

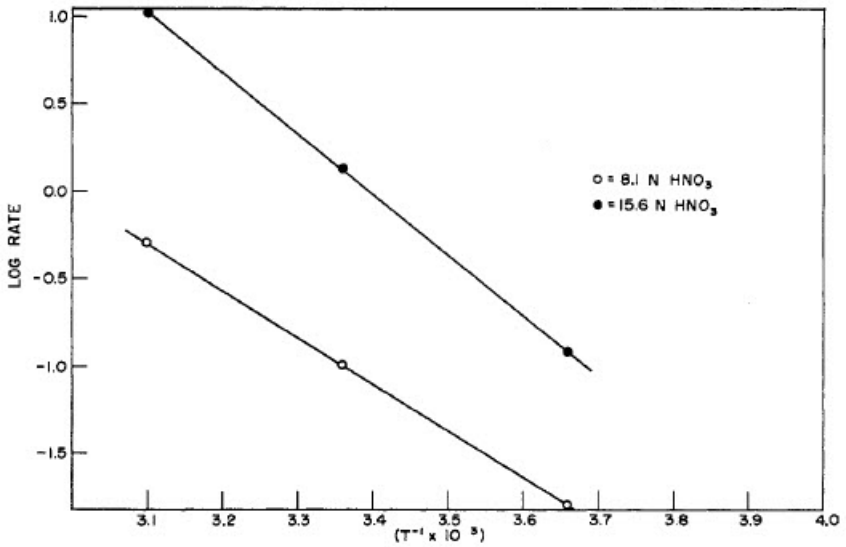

Figure 1-2. Calculation of Activation Energies for U Metal Dissolutions

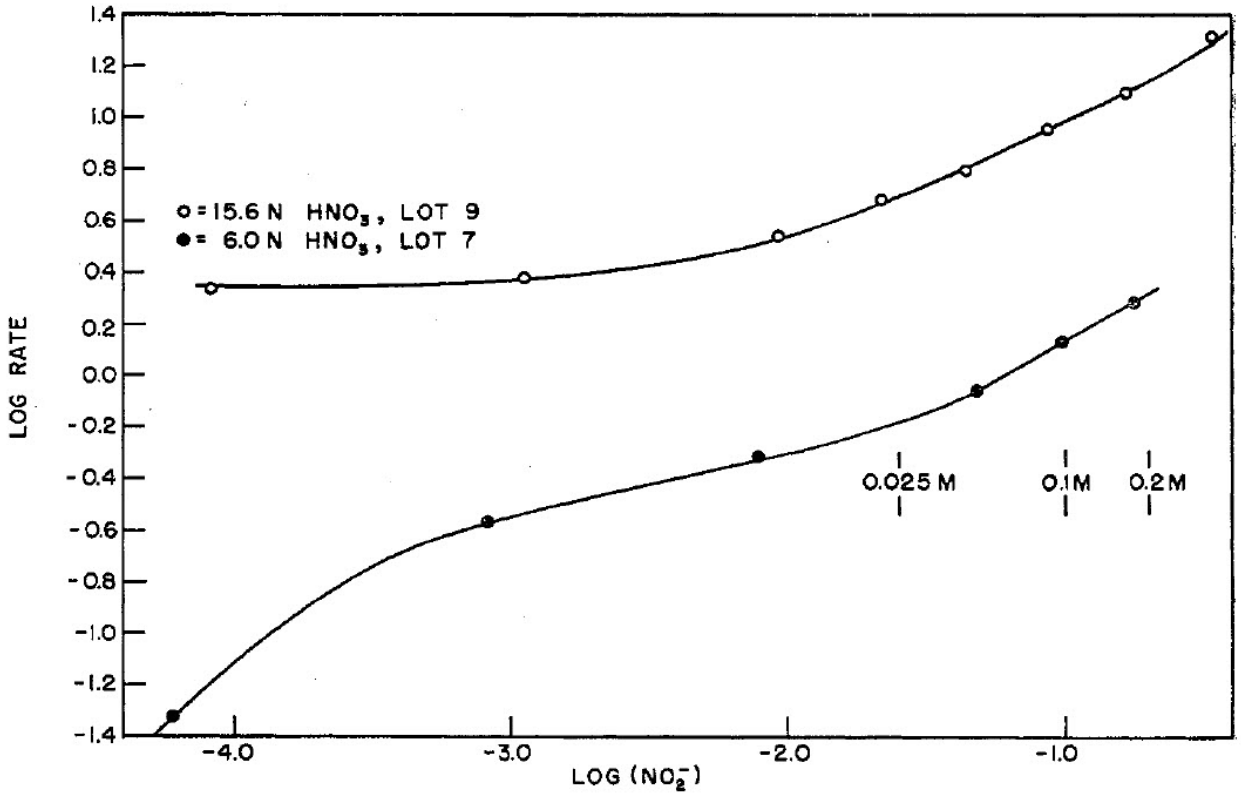

Figure 1-3. Enhancement of U Metal Dissolution Rate by the Addition of KNO_2

The dissolution of U metal is catalyzed by materials other than HNO_2. The use of phosphoric acid (H_3PO_4) as a catalyst was demonstrated in the early 1950's. The effect of H_3PO_4 on the rate of dissolution of U metal in HNO_3 was determined as a function of the concentrations of phosphate (PO_4^{3-}), HNO_3, and $UO_2(NO_3)_2$.[9] Small concentrations of PO_4^{3-}, in the range of 0.01 to 0.15 M, significantly increased the rate of attack on

the metal, particularly at high acidities. Higher PO_4^{3-} concentrations inhibited the dissolution of U metal with the effect being most pronounced at low HNO_3 concentrations (Figure 1-4).

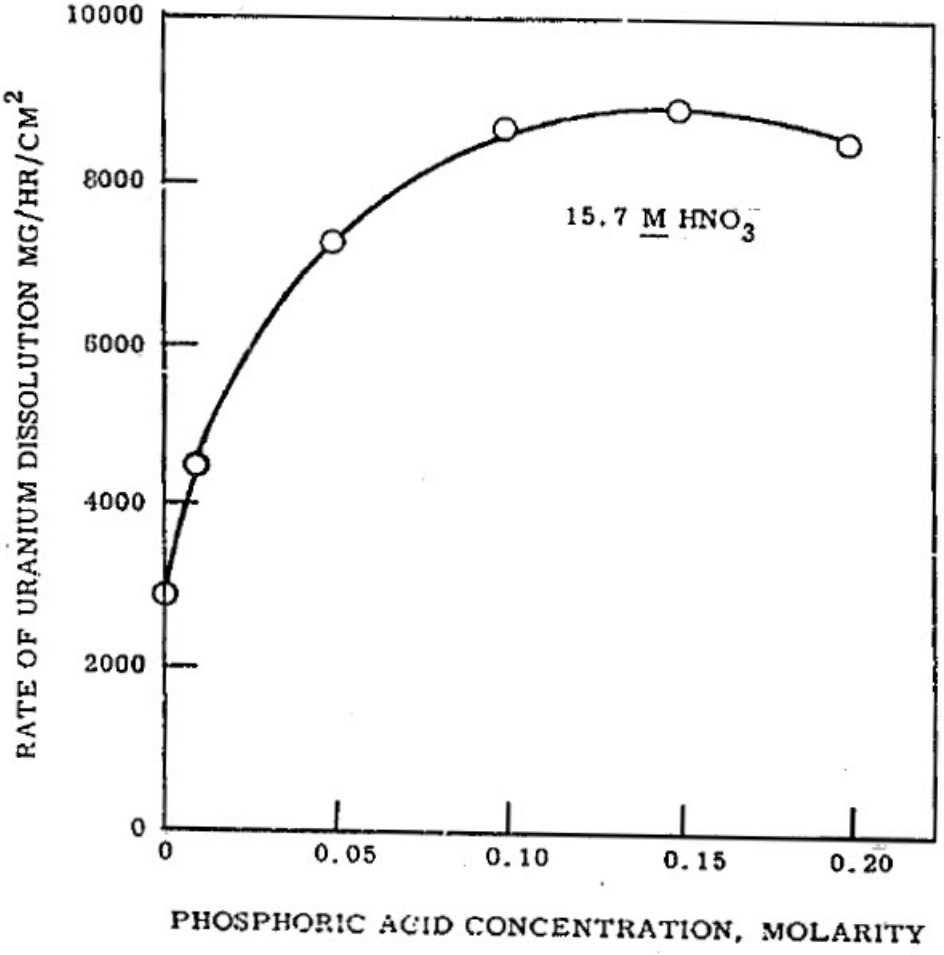

Figure 1-4. Rate of U Metal Dissolution with Phosphoric Acid Catalysis

Uranium metal dissolutions are also catalyzed by the presence of fluoride in the solution. Pierce measured the dissolution rate of pieces of U metal sheet in a series of experiments using varying concentrations of HNO_3 and fluoride.[10] The fluoride was added as KF. In most of the dissolutions, the solution also contained 2 g/L B which would limit the concentration of free fluoride due to complexation. Table 1-1 shows U metal dissolution rates measured at 2 and 4 M HNO_3 containing fluoride concentrations from 0 to 0.1 M at room temperature to approximately the boiling point of the solution. The data in the table show that the effect of increasing fluoride concentration is much more pronounced than the effect of increasing the HNO_3 concentration with the dissolution rates increasing by greater than an order of magnitude at both acid concentrations when the fluoride concentration increases from 0 to 0.1 M.

Table 1-1. U Metal Dissolution Rates in HNO_3 Solutions Containing Fluoride

Solution Composition			Dissolution Rate (mg/min·cm^2)				
HNO_3 (M)	KF (M)	B (g/L)	20-25 (˚C)	50 (˚C)	60 (˚C)	80 (˚C)	100 (˚C)
2	0	0	–	–	nd	0.007	0.051
2	0.01	2	0.099	0.308	–	–	1.07
2	0.025	2	0.137	0.540	–	–	2.35
2	0.05	2	–	–	–	–	6.48
2	0.1	2	–	–	–	–	12.6
2	0.1	0	0.213	–	–	–	18.5
4	0	0	–	–	0.003	0.041	0.309
4	0.01	2	0.097	0.293	–	–	1.31
4	0.025	2	0.097	0.370	–	–	3.16
4	0.05	2	–	–	–	–	6.48
4	0.1	2	0.541	–	–	–	20.5

nd – not detected

Pierce also measured U metal dissolution rates in a series of experiments without the presence of fluoride at varying HNO_3 and total nitrate concentrations.[10] The dissolution rates (Table 1-2) increased with increasing HNO_3 concentration which is consistent with the observations of Lacher et al.[3] (Figure 1-1); although, experiments were not performed at sufficiently high acid concentrations where the dissolution rate begins to decrease. The dissolutions rates measured at total nitrate concentrations of 4 and 7 M were similar; although, the HNO_3 concentration varied, which is consistent with the laboratory studies described by Colven et al. which noted that at a given total nitrate concentration, the dissolution rate is independent of the HNO_3 or the U (i.e., metal nitrate) concentrations.[5]

Table 1-2. U Metal Dissolution Rates in HNO_3 Solution

Solution Composition			Dissolution Rate (mg/min·cm^2)				
HNO_3 (M)	$NaNO_3$ (M)	Total Nitrate (M)	20-25 (˚C)	60 (˚C)	65 (˚C)	80 (˚C)	100 (˚C)
2	0	2	–	nd	–	0.007	0.051
2	2	4	–	–	–	–	0.254
4	0	4	–	–	0.003	0.041	0.309
4	3	7	–	–	–	–	1.26
7	0	7	0.005	–	0.074	0.841	1.28
10	0	10	–	–	1.637	3.50	4.06

nd – not detected

A dissolution flowsheet for low enriched U (LEU) metal ingots from the electrometallurgical treatment of fuel from the Experimental Breeder Reactor-II (EBR-II) was developed by Daniel et al. for potential use in the Savannah River Site H-Canyon facility.[11] The flowsheet was designed to allow the dissolution of a batch of Al-clad research reactor fuel using existing flowsheets followed by the dissolution of the LEU metal. In a laboratory-scale demonstration of the flowsheet, the rate of dissolution of the metal in a 1.4 M HNO_3 solution containing 0.002 M Hg and 1.6 M Al at the boiling point was 4.7 mg/min/cm^2. During the development of the dissolution flowsheet, the offgas from the dissolution of the U metal was measured and characterized by mass spectrometry and Raman spectroscopy. The H_2 generation rate from samples of the metal were shown to be inconsequential; therefore, the dissolution of the metal had no significant impact on the generation of H_2.

2.0 Experimental Procedure

2.1 LEU Metal

The LEU metal used in the dissolution experiments was produced by electrometallurgical processing of fast reactor fuel from the EBR-II at the Idaho National Laboratory (INL).[12] The samples were taken from molten U metal in the cathode processor by vacuum casting into small sample rods using a glass mold. Characterization data for the U metal are shown in Table 2-1.[13]

Table 2-1. Characterization Data for LEU Samples

Element	Units	Mean Value[(a)]
Al	ppm	<180
Cd	ppm	<15
C	ppm	~220
Cr	ppm	<50
Fe	ppm	123
Li	ppm	<10
Mn	ppm	14
Mo	ppm	<90
Ni	ppm	<20
N	ppm	<5
O	ppm	~130
Si	ppm	~125
Zr	ppm	681
Total U	wt %	99.9
U-235	wt %	19.7

(a) Mean value for two ingots

The LEU sample rods had an approximate 3 mm diameter and were cut to lengths of approximately 25 mm. The cut samples were wiped clean and then weighed and measured prior to the dissolution. The surface area of the LEU samples was based on the diameter and length as shown by equation 3,

$$\mathrm{SA}\left(\mathrm{cm}^2\right) = 2 \cdot \pi \cdot \left[\frac{d(\mathrm{cm})}{2}\right]^2 + \pi \cdot \mathrm{d(cm)} \cdot \ell(\mathrm{cm}) \quad (3)$$

where SA is the surface area of the immersed coupon, d is the diameter of the coupon, and ℓ is the length of the coupon. The masses, dimensions, and surface areas of the LEU samples used in the experiments are provided in Table 2-2.

Table 2-2. LEU Sample Characteristics

Exp. No.	Mass (g)	Length (mm)	Diameter (mm)	Surface Area (cm^2)
125	2.8434	26.83	2.86	2.539
126	3.0545	26.78	2.87	2.544
127	3.1591	26.81	2.86	2.537
128	3.2086	26.93	2.86	2.548
129	3.1527	27.00	2.86	2.554
130	3.0186	25.81	2.88	2.466
131	3.0525	25.77	2.86	2.444
132	2.1868	18.60	2.85	1.793
134	3.4875	29.73	2.87	2.810
135	3.2671	38.66	2.86	3.602

2.2 Dissolving System

The vessel and offgas condenser used to perform the LEU dissolution experiments were fabricated from borosilicate glass by the SRNL Glass Shop. The dissolving vessel was made from a 300-mL round-bottom flask. Penetrations were added for a condenser, Hg addition (which was not used in this work), thermocouple, and gas purge. The bottom of the flask was flattened slightly to facilitate heating and agitation using a hot plate/stirrer with a magnetic stir bar. During dissolution, the LEU sample was charged to the dissolver in a glass basket suspended by a glass rod which was held in place by a compression fitting. The compression fitting allows adjustment of the basket height during dissolution. The solution temperature was controlled using an external thermocouple monitored by the hot plate. Offgas exiting the dissolving vessel can be sampled for analysis using a sample line connected to a port just above the condenser. A manometer, also connected to the offgas sample port, acts as a pressure relief device and provides a measurement of the pressure in the system. The offgas leaving the condenser passes through a cell containing a Raman probe and terminates in a bubbler (i.e., beaker containing 700 mL or 3.5 in of deionized water). The bubbler prevents air in-leakage from the vent side of the system. The Raman spectrometer is used to measure non-condensable gases such as H_2, N_2, O_2, CO_2, NO, N_2O and NO_2 in real time during the experiment. Photographs of the equipment are shown in Figure 2-1.

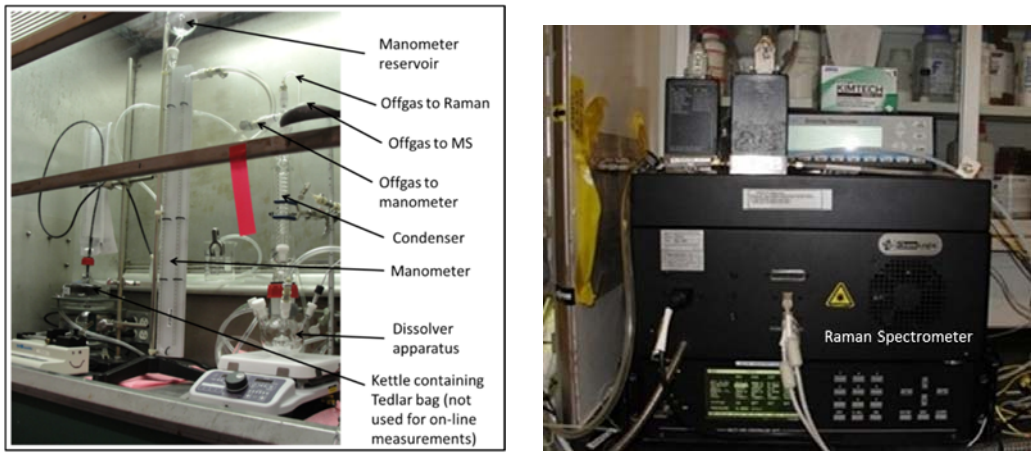

Figure 2-1. Dissolver Setup with Online Raman Offgas Analyzer

The glass dissolver used in the experiments in which NO gas was sparged into the solution is shown in Figure 2-2. In these experiments, a penetration was added for the NO gas and the vessel was equipped with a fritted disk positioned below the basket holding the U metal sample to allow sparging the solution. The

penetrations in the vessel for the hot plate thermocouple and purge/tracer gas inlet were used for the same functions as in the other series of experiments. The solution in the bubbler was replaced with 3 M NaOH to neutralize the small amount of NO gas flowing through the system.

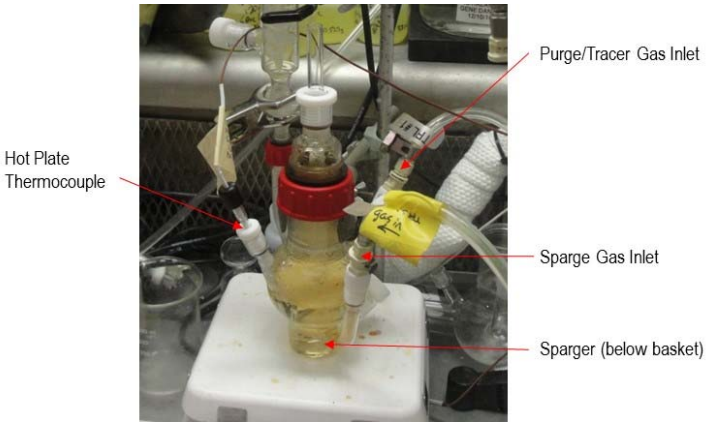

Figure 2-2. Dissolver Setup with Sparger below Coupon Basket

2.2.1 Sparger Gas Setup

For two experiments, NO gas was metered into the system through a sparger just below the glass basket at a set rate (calibrated at 70 ˚F and 1 atm). The intent of the experiments was to saturate the solution with NO gas since the reaction of U metal with HNO_3 is autocatalytic, as factors which increase the concentrations of the gaseous reaction products also increase the dissolution rate. The presence of NO gas in solution will also generate both NO_2 gas and HNO_2 which are in equilibrium with the NO gas (equation 1 and 2). The presence of HNO_2 is most likely responsible for the catalytic effect.[3] In the initial experiment, the sparge rate of NO gas was controlled at 50 cm^3/min. Based on a solution volume of 120 mL in the dissolution vessel, the NO gas had a residence time of 2.4 min following saturation of the solution. In the second experiment, a smaller flowrate of NO gas, 35 cm^3/min, was used which had a residence time of 3.4 min.

2.3 Dissolution Experiments

To perform a dissolution experiment, the U sample was initially placed in the perforated glass basket and suspended above the solution. The solution was heated to the desired temperature. Chilled water (at 4 ˚C) was circulated through the condenser during the dissolution to remove water vapor from the offgas stream. Once the solution reached the desired temperature, the basket with the sample was lowered until it was completely immersed. A timer was started to record the time the sample went into solution. At the desired interval, the basket was raised out of solution, the timer stopped, and the basket was removed from the dissolving vessel. The sample was then removed from the basket, dried, and weighed and the dimensions (i.e., length and diameter) measured. The sample was then returned to the basket and the basket lowered back into the solution. The timer was started again. This process was repeated until the sample was too small to remove and acquire meaningful data.

In the first two series of experiments, the effects of the HNO_3 concentration and the dissolving temperature on the U metal dissolution rate were evaluated. Additional experiments were performed to examine the catalytic effects of fluoride and NO gas on the dissolution rate. The experimental conditions are provided in Table 2-3.

Table 2-3. Experimental Matrix

Exp. No.	Nitric Acid Concentration	Dissolution Temperature	Fluoride Concentration	NO Sparge rate
	(M)	(˚C)	(M)	(cm^3/min)*
125	4	103	0	0
126	6	107	0	0
127	8	110	0	0
128	10	113	0	0
129	8	100	0	0
130	8	90	0	0
131	8	90	0.01	0
132	4	103	0.01, 0.05, 0.1	0
133	8	100	0	50
134	8	100	0	35

* 70 ˚F and 14.6 psia

2.4 Quality Assurance

Requirements for performing reviews of technical reports and the extent of review are established in manual E7 2.60. SRNL documents the extent and type of review using the SRNL Technical Report Design Checklist contained in WSRC-IM-2002-00011, Rev. 2.

3.0 Results and Discussion

3.1 Dissolution of U Metal Samples

Samples of LEU metal ingots produced by electrometallurgical processing of fast reactor fuel from the EBR-II at the INL were dissolved in solutions of 4, 6, 8, and 10 M HNO_3 at the boiling point. Additional dissolutions were performed using 8 M HNO_3 at 100 ˚C and 90 ˚C to examine the effect of temperature at a constant acid concentration. The catalytic effects of fluoride and NO gas were subsequently examined in separate series of experiments.

3.1.1 Effect of HNO_3 Concentration

The instantaneous dissolution rate of the U metal samples was measured by periodically removing the sample from the dissolving solution and measuring the mass and physical dimensions (i.e., diameter and length) and then returning the sample to the solution.

Table 3-1, Table 3-2, Table 3-3, and Table 3-4 provide the masses and dimensions of the samples as functions of time in Experiment 125 using 4 M HNO_3 at boiling (103 ˚C), Experiment 126 using 6 M HNO_3 at boiling (107 ˚C), Experiment 127 using 8 M HNO_3 at boiling (110 ˚C), and Experiment 128 using 10 M HNO_3 at boiling (113 ˚C), respectively.

The dissolution rates of the U metal were calculated using plots of the mass-to-surface area ratio and the dissolution time for Experiments 125-128 (Figure 3-1). Data from a previous experiment (Experiment 79) performed using 7 M HNO_3 at boiling (110 ˚C)[11] are also shown in Figure 3-1 for comparison. The measured dissolution rate is obtained as the slope of a linear regression of the mass-to-surface area ratio versus time. Note that the initial and last data point(s) for the experiments are generally not used in the regression due to an initial induction period and the tailing-off observed at the end of the dissolution. The induction period is due to the removal of oxide from the U metal surface. The tailing-off is likely due to the difficulty in accurately calculating the surface area when the sample is nearly dissolved.

Based on the linear regressions, the dissolution rates for the U metal samples at the various HNO_3 concentrations (at the boiling point) are shown in Table 3-5. The calculated values show that the dissolution rate increases with increasing HNO_3 concentration as expected. Increasing the HNO_3 concentration from 4 to 6 M more than doubled the dissolution rate while increases from 4 to 8 M and 4 to 10 M increased the dissolution rate by almost 7 and 12 times, respectively. Based on the work by Lacher et al.,[3] increases in the U metal dissolution rate would be expected to continue until the HNO_3 concentration reaches 13-14 M (Figure 1-1). In this concentration range, the rate is expected to begin to decrease due to the passivation (i.e., oxidation) of the metal surface by the highly oxidizing solution. The optimum HNO_3 concentration for a U metal dissolution process depends upon the desired cycle time and the acid concentration required for downstream processing. We chose not to dissolve at an acid concentration higher than 10 M due to the potential use of an ammonium diuranate (ADU) precipitation process to isolate the U following dissolution. Excess acid must be neutralized during the precipitation process and higher concentrations used during dissolution would generate higher volumes of liquid waste.

Table 3-1. Exp 125 – U Metal Dissolution Rate Data for 4 M HNO_3 at Boiling (103 ˚C)

Time (min)	Mass (g)	Diameter (mm)	Length (mm)	Surface Area (SA) (cm^2)	Mass/SA (mg/cm^2)
0.0	3.1778	2.86	26.83	2.539	1251.52
35.1	3.1345	2.85	26.93	2.539	1234.65
65.7	3.054	2.83	26.37	2.470	1236.30
97.7	2.6918	2.77	26.35	2.414	1115.28
131.4	2.2709	2.59	25.75	2.201	1031.96
163.6	1.9441	2.42	25.61	2.039	953.44
194.1	1.6841	2.2	25.42	1.833	918.80
224.4	1.4677	2.03	25.36	1.682	872.57
258.6	1.2548	1.96	25.53	1.632	768.70
289.4	1.083	1.8	25.38	1.486	728.75
1136.4	0	0	0	0	0

Table 3-2. Exp 126 – U Metal Dissolution Rate Data for 6 M HNO_3 at Boiling (107 ˚C)

Time (min)	Mass (g)	Diameter (mm)	Length (mm)	Surface Area (SA) (cm^2)	Mass/SA (mg/cm^2)
0.0	3.0545	2.87	26.78	2.544	1200.68
30.32	2.9443	2.85	26.31	2.483	1185.66
60.97	2.0332	2.62	25.77	2.229	912.35
91.43	1.2003	2.09	23.16	1.589	755.25
126.35	0.6324	1.66	20.91	1.134	557.79
156.65	0.3237	1.22	20.26	0.800	404.68
186.90	0.1298	0.85	19.725	0.538	241.23
280.52	0	0	0	0	0

Table 3-3. Exp 127 – U Metal Dissolution Rate Data for 8 M HNO_3 at Boiling (110 ˚C)

Time (min)	Mass (g)	Diameter (mm)	Length (mm)	Surface Area (SA) (cm^2)	Mass/SA (mg/cm^2)
0.0	3.1591	2.86	26.81	2.537	1245.04
30.3	1.972	2.34	25.96	1.994	988.76
53.2	0.908	1.75	25.37	1.443	629.29
66.4	0.4761	1.32	25.15	1.070	444.82
111.9	0	0	0	0	0

Table 3-4. Exp 126 – U Metal Dissolution Rate Data for 10 M HNO_3 at Boiling (113 ˚C)

Time (min)	Mass (g)	Diameter (mm)	Length (mm)	Surface Area (SA) (cm^2)	Mass/SA (mg/cm^2)
0.0	3.2086	2.86	26.93	2.548	1259.20
8.4	2.4125	2.65	26.57	2.322	1038.83
13.3	1.7662	2.23	26.41	1.928	915.92
18.4	1.2318	1.96	26.04	1.664	740.37
23.3	0.8165	1.57	25.53	1.298	629.08
28.3	0.486	1.21	25.56	0.995	488.63
34.5	0.2107	0.77	25.09	0.616	341.91
47.8	0	0	0	0	0

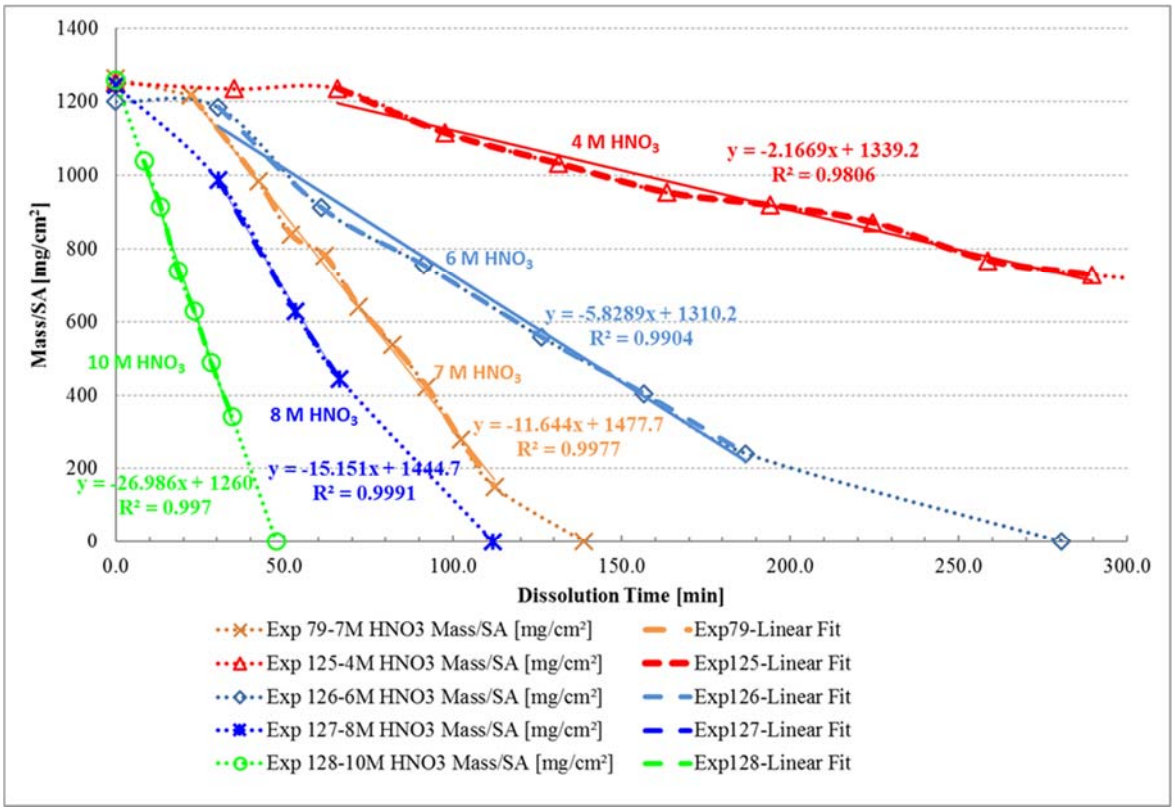

Figure 3-1. Calculation of U Metal Dissolution Rate as a Function of the HNO_3 Concentration

Table 3-5. U Metal Dissolution Rate at Boiling as a Function of HNO_3 Concentration

Exp. No.	Nitric Acid Concentration	Dissolution Temperature	Dissolution Rate
	(M)	(˚C)	(mg/cm^2/min)
125	4	103	2.2
126	6	107	5.8
127	8	110	15.2
128	10	113	27.0

3.1.2 Effect of Temperature

To examine the effect of temperature on the dissolution rate, 8 M HNO_3 was selected as the target concentration, since the dissolution rate of U metal at boiling was fast enough that dissolutions performed at 100 ˚C and 90 ˚C could be completed in a reasonable amount of time. Table 3-6 and Table 3-7 provide the masses and dimensions of the U metal samples as functions of time in Experiment 129 using 8 M HNO_3 at 100 ˚C and Experiment 130 using 8 M HNO_3 at 90 ˚C, respectively. Plots of the mass-to-surface area ratio versus dissolution time for Experiments 127, 129, and 130 are shown in Figure 3-2. The measured dissolution rate was obtained as the slope of a linear regression of the mass-to-surface area ratio versus time. The initial and last point(s) were generally not used in the regression due to the initial induction period and the tailing-off period toward the end of the dissolutions. Based on the linear regressions, the dissolution rates for the U metal samples at the three temperatures are shown in Table 3-8. The calculated values show that the dissolution rate increases with increasing temperature as expected. A reduction in temperature from 110 ˚C to 100 ˚C, results in a reduction in the dissolution rate by a factor of two. However, a reduction in temperature from 100 ˚C to 90 ˚C only reduces the dissolution rate by about 10%. This temperature effect illustrates that U metal dissolution in HNO_3 is not an extremely strong function of temperature. Even though the dependence on temperature is not very strong, performing the dissolution at the boiling point is recommended to maximize the dissolution rate, unless there is a valid reason (i.e., process safety) to perform the dissolution at a lower temperature.

Table 3-6. Exp 129 – U Metal Dissolution Rate Data for 8 M HNO_3 at 100 ˚C

Time (min)	Mass (g)	Diameter (mm)	Length (mm)	Surface Area (SA) (cm^2)	Mass/SA (mg/cm^2)
0.0	3.1527	2.86	27	2.554	1234.21
15.4	2.95	2.72	26.33	2.366	1246.75
30.5	2.6206	2.81	26.13	2.431	1078.10
45.7	2.0783	2.58	25.84	2.199	945.12
60.9	1.5466	2.15	25.42	1.790	864.22
76.1	1.0986	1.76	24.93	1.427	769.82
91.4	0.7357	1.47	24.88	1.183	621.93
106.5	0.4511	1.24	24.21	0.970	465.08
121.7	0.2364	0.91	23.82	0.694	340.64
171.2	0	0	0	0	0

Table 3-7. Exp 130 – U Metal Dissolution Rate Data for 8 M HNO_3 at 90 ˚C

Time (min)	Mass (g)	Diameter (mm)	Length (mm)	Surface Area (SA) (cm^2)	Mass/SA (mg/cm^2)
0.0	3.0186	2.88	25.81	2.466	1224.32
15.9	2.9215	2.82	25.44	2.379	1228.18
31.8	2.8304	2.79	25.32	2.342	1208.76
47.5	2.7055	2.76	25.14	2.299	1176.56
62.7	2.4986	2.7	24.92	2.228	1121.30
78.0	2.1261	2.58	24.52	2.092	1016.31
93.3	1.6906	2.32	24.03	1.836	920.82
109.0	1.2853	2.01	24.03	1.581	813.04
124.6	0.9394	1.86	23.61	1.434	655.11
140.7	0.6355	1.52	23.39	1.153	551.07
156.3	0.4012	1.27	23.03	0.944	424.91
172.2	0.2189	0.91	22.87	0.667	328.27

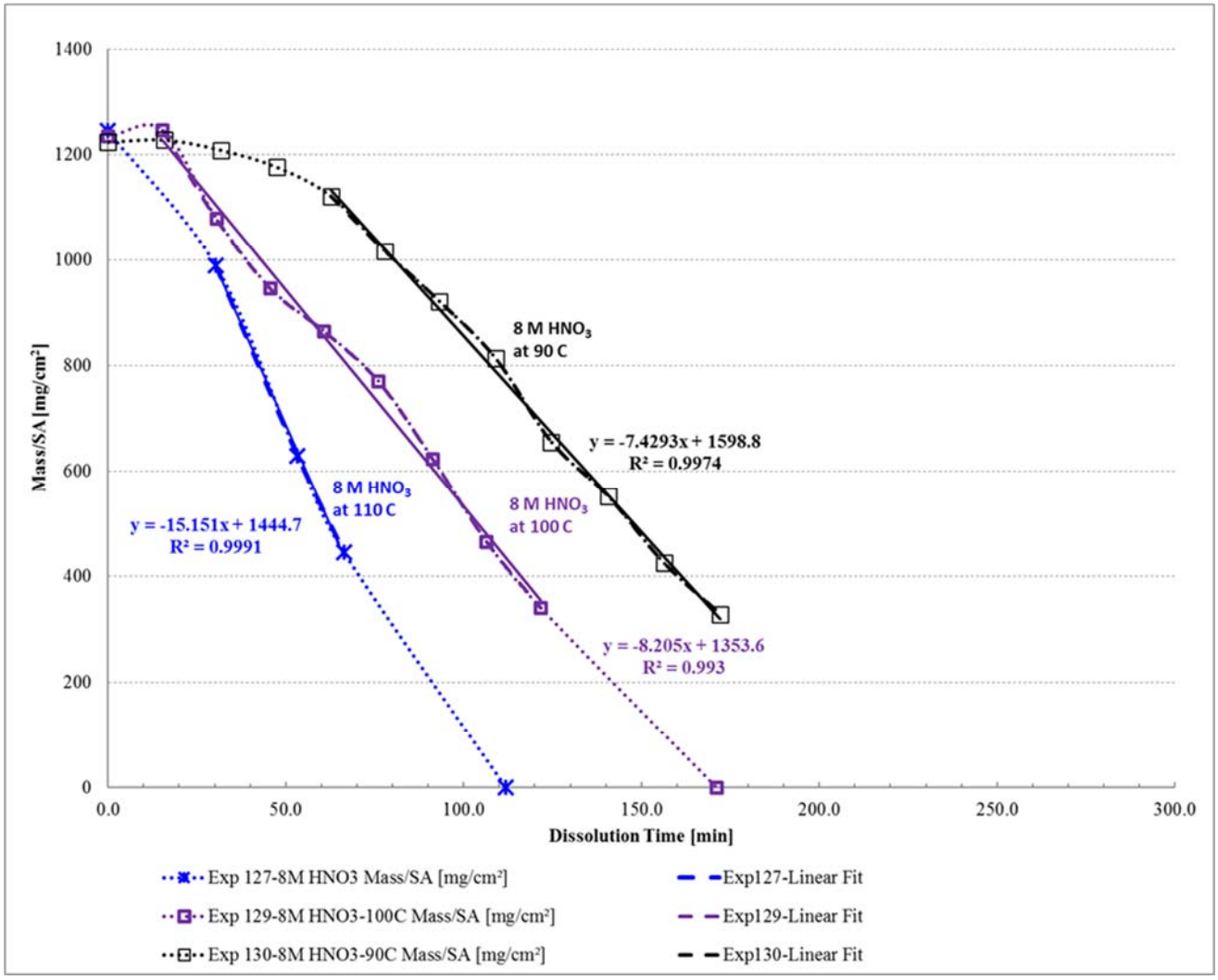

Figure 3-2. Calculation of U Metal Dissolution Rate as a Function of Temperature

Table 3-8. U Metal Dissolution Rates at 8 M HNO_3 as Function of Temperature

Exp. No.	Dissolution Temperature	Dissolution Rate
	(˚C)	(mg/cm^2/min)
127	110	15.2
129	100	8.2
130	90	7.4

3.1.3 Fluoride Catalysis

In response to a request from the General Atomics team, experiments were performed to examine the impact of fluoride ion on the dissolution rate of U metal. Prior studies have shown that the presence of fluoride has a dramatic effect on the dissolution rate.[10] For the initial experiment, an 8 M HNO_3 solution containing 0.01 M fluoride at 90 ˚C was used for the dissolution. The low concentration of fluoride was expected to provide a significant and easily measurable increase in the dissolution rate. In addition, minimizing the fluoride concentration was desired to facilitate the removal of the ion during the ADU precipitation process proposed to isolate the U prior to conversion to UO_2 for the ^{99}Mo production target.

Table 3-9 provides the masses and dimensions of the U metal sample as a function of time for Experiment 131 in which an 8 M HNO_3 solution containing 0.01 M fluoride at 90 ˚C was used to dissolve the metal. Experiment 131 was a duplication of Experiment 130 with the addition of 0.01 M fluoride to examine its catalytic effect below the boiling point of the solution. Plots of the mass-to-surface area ratio versus dissolution time for Experiments 130 and 131 are shown on Figure 3-3. The dissolution rate measured in Experiment 131 was 8.5 mg/cm^2/min compared to 7.4 mg/cm^2/min measured in Experiment 130 which is only about a 15% increase. The increase in the dissolution rate was not as large as anticipated; therefore, additional experiments were performed to examine the effect of fluoride at higher temperature.

Table 3-9. Exp 131 – U Metal Dissolution Data for 8 M HNO_3/0.01 M Fluoride at 90 ˚C

Time (min)	Mass (g)	Diameter (mm)	Length (mm)	Surface Area (SA) (cm^2)	Mass/SA (mg/cm^2)
0.0	3.0525	2.86	25.77	2.444	1249.02
5.2	3.0037	2.83	26.16	2.452	1225.19
10.4	2.9567	2.82	25.9	2.419	1222.04
15.6	2.8832	2.83	25.44	2.388	1207.57
24.8	2.5437	2.74	25.36	2.301	1105.52
30.1	2.2811	2.68	25.42	2.253	1012.45
35.5	2.0423	2.49	25.15	2.065	989.12
45.6	1.6764	2.22	24.91	1.815	923.78
55.9	1.3667	2.04	24.77	1.653	826.88
66.1	1.0989	1.81	24.36	1.437	764.91
77.0	0.846	1.65	24.48	1.312	644.96
87.8	0.62	1.43	24.27	1.122	552.37
98.0	0.4405	1.21	24.16	0.941	467.92
108.4	0.2897	0.91	23.89	0.696	416.24
118.6	0.1673	0.79	23.71	0.598	279.65

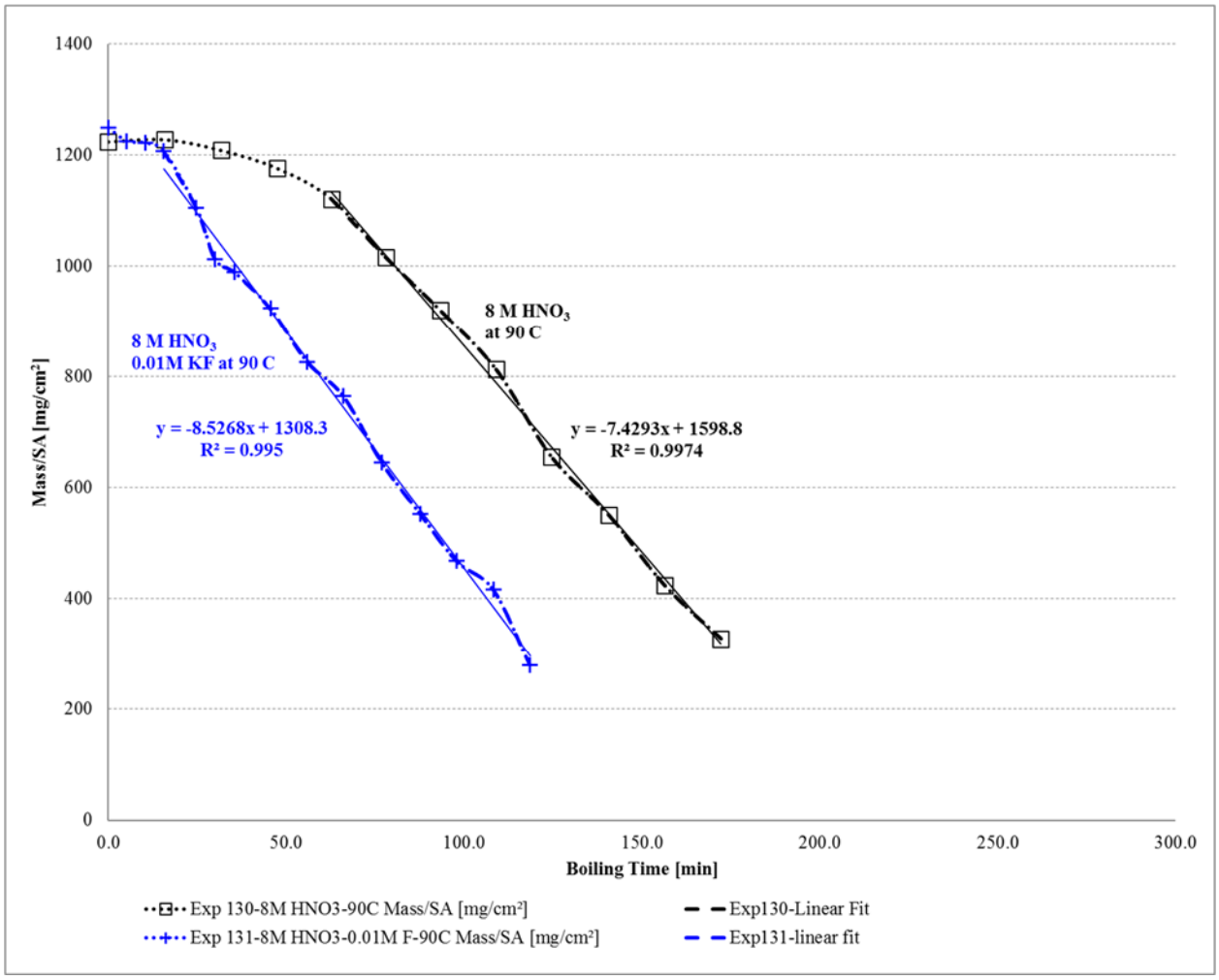

Figure 3-3. Effect of Fluoride on the Sub-boiling U Metal Dissolution Rate

To examine the catalytic effect of fluoride at higher temperature on the U metal dissolution rate, Experiment 132 was performed using a 4 M HNO_3 solution containing 0.01 M fluoride at the boiling point (103 ˚C). Table 3-10 provides the masses and dimensions of the U metal sample as a function of time. A plot of the mass-to-surface area ratio versus dissolution time for Experiment 132 is shown in Figure 3-4. The measured dissolution rate with the solution containing 0.01 M fluoride (1.7 mg/cm^2/min) was about the same as without fluoride (2.2 mg/cm^2/min). In response to the slower than expected dissolution rate, the experiment was stopped and the 0.01 M fluoride in the (120 mL) dissolving solution was increased to 0.05 M fluoride by adding 10 mL of a 4 M HNO_3 solution containing 0.53 M KF. The dissolution experiment was re-started (Experiment 132A) and the mass and dimensions of the U metal sample were measured as a function of time (Table 3-11). A plot of the mass-to-surface area ratio versus dissolution time for Experiment 132A is shown in Figure 3-4. The measured dissolution rate using 0.05 M fluoride (3.9 mg/cm^2/min) was about twice the rate measured using 0.01 M fluoride (1.7 mg/cm^2/min). The experiment was subsequently stopped and the (130 mL) 0.05 M fluoride solution was increased to 0.1 M fluoride by adding 10 mL of a 4 M HNO_3 solution containing 0.75 M KF. The experiment was re-started (Experiment 132B) and the mass and dimensions of the U metal sample were measured over time (Table 3-12). A plot of the mass-to-surface area ratio versus dissolution time for Experiment 132B is shown in Figure 3-4. The measured dissolution rate using 0.1 M fluoride (16.7 mg/cm^2/min) was more than four times the rate measured using 0.05 M fluoride (3.9 mg/cm^2/min) and was about ten times the rate measured using 0.01 M fluoride

(1.7 mg/cm^2/min). The dissolution rate using 4 M HNO_3 containing 0.1 M fluoride is reasonably consistent with values measured by Pierce using 2 M (18 mg/cm^2/min) and 4 M (20 mg/cm^2/min) HNO_3 containing the same concentration of fluoride.[10] The difference in the dissolution rates using 4 M HNO_3 are likely attributed to factors inherent to the U used in the dissolution studies (e.g., impurities, metal treatment, grain size, and shape).

Table 3-10. Exp 132 – U Metal Dissolution Rate Data for 4 M HNO_3/0.01 M Fluoride at Boiling

Time (min)	Mass (g)	Diameter (mm)	Length (mm)	Surface Area (SA) (cm^2)	Mass/SA (mg/cm^2)
0.0	2.1868	2.85	18.6	1.793	1219.67
15.1	2.1215	2.81	18.58	1.764	1202.49
30.2	2.0549	2.78	18.5	1.737	1182.94
44.1	1.9789	2.8	18.53	1.753	1128.78
58.9	1.8955	2.78	18.2	1.711	1107.89
74.1	1.8185	2.69	18.34	1.664	1093.14
89.1	1.7287	2.76	17.95	1.676	1031.40
104.0	1.6499	2.63	17.86	1.584	1041.40
119.1	1.5734	2.53	17.95	1.527	1030.22

Table 3-11. Exp 132A – U Metal Dissolution Rate Data for 4 M HNO_3/0.05 M Fluoride at Boiling

Time (min)	Mass (g)	Diameter (mm)	Length (mm)	Surface Area (SA) (cm^2)	Mass/SA (mg/cm^2)
0.0	1.5734	2.53	17.95	1.527	1030.22
15.1	1.2929	2.24	17.44	1.306	989.89
19.9	1.2257	2.2	17.3	1.272	963.82
25.0	1.1585	2.16	17.15	1.237	936.50
30.0	1.0986	2.12	17.18	1.215	904.33
40.1	0.9869	2.01	17.05	1.140	865.62
50.2	0.8884	1.89	16.88	1.058	839.40
60.3	0.7927	1.81	16.43	0.986	804.19
70.6	0.7068	1.73	16.5	0.944	748.90
80.7	0.6279	1.61	16.54	0.877	715.72
91.1	0.5530	1.51	16.43	0.815	678.34
102.0	0.4820	1.42	16.13	0.751	641.60

Table 3-12. Exp 132B – U Metal Dissolution Rate Data for 4 M HNO_3/0.1 M Fluoride at Boiling

Time (min)	Mass (g)	Diameter (mm)	Length (mm)	Surface Area (SA) (cm^2)	Mass/SA (mg/cm^2)
0.0	0.482	1.42	16.13	0.751	641.60
10.0	0.2898	1.1	15.84	0.566	511.65
15.1	0.2108	0.91	15.77	0.464	454.46
20.1	0.1455	0.81	15.49	0.404	359.72
40.2	0	0	0	0	0

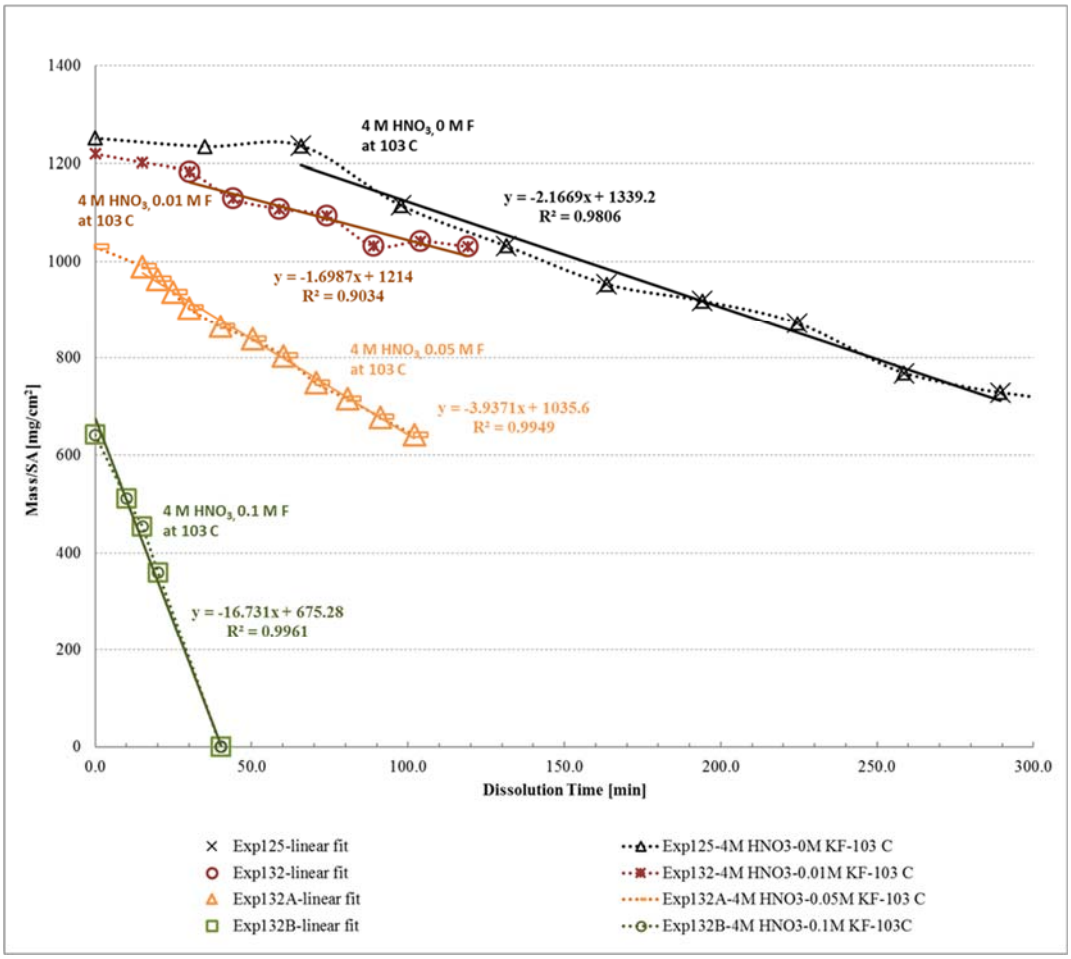

Figure 3-4. Calculation of U Metal Dissolution Rate as a Function of Fluoride Concentration

The ineffectiveness of 0.01 M fluoride in catalyzing the U metal dissolutions in Experiments 131 and 132 is likely due to the complexation of the fluoride by the U in solution. Stability constants for the complexation of fluoride by UO_2^{2+} have been published for one to four fluorides per UO_2^{2+} molecule. The largest stability constant reported is for the difluoro complex ($\beta_2 = 112$) measured in 1 M $NaClO_4$ at 20 ˚C (equation 4).[14]

$$UO_2^{2+} + 2HF \rightleftharpoons UO_2F_2 + 2H^+ \quad (4)$$

Table 3-13 provides a summary of the dissolution rates measured using 4 M HNO_3 at the boiling point of the solution as a function of the fluoride concentration. The table also includes the fluoride to U molar ratio at the completion of the dissolution. For the fluoride to have a significant effect on the dissolution rate, a concentration greater than 0.01 M was required. The data also show that a fluoride to U molar ratio near or greater than one was necessary to provide sufficient free fluoride to effectively catalyze the dissolution.

Table 3-13. U Metal Dissolution Rates at 4 M HNO_3 as a Function of Fluoride Concentration

Exp. No.	Fluoride	Fluoride to U Ratio	Dissolution Rate
---	(M)	(mol/mol)	($mg/cm^2/min$)
125	0.0	0	2.2
132	0.01	0.1	1.7
132A	0.05	0.9	3.9
132B	0.10	3.0	16.7

If fluoride is used to catalyze the dissolution of U metal, the effect of fluoride on the preparation of UO_2 target material should be considered. Following metal dissolution, the General Atomic flowsheet isolates the U by an ADU precipitation process. Although, fluoride is soluble in the precipitation process, decontamination factors for soluble species during precipitations are generally low without significant washing of the precipitate which adds to the waste volume. Kyser measured the decontamination factor (i.e., the ratio of the concentration of fluoride in the feed to the product) in a Pu(IV) oxalate precipitation followed by filtration and calcination to PuO_2.[15] The fluoride concentration in the feed to the precipitation process was nominally 0.1 M (1.9 g/L). The oxalate precipitate was only washed with a portion of the filtrate to ensure that solids were removed from the precipitation vessel. The decontamination factor obtained in the laboratory-scale processes was only five. Therefore, the use of fluoride to catalyze U metal dissolution must be balanced against the potential for corrosion of downstream equipment and the addition of corrosion products to the U product stream.

3.1.4 NO Catalysis

To examine the impact of sparging NO gas into the HNO_3 solution during dissolution, the dissolver system was modified to allow the introduction of NO just below the coupon basket containing the U metal. The presence of NO in solution will generate both NO_2 gas and HNO_2 which are in equilibrium with the NO (equations 1 and 2). The generation of increased concentrations of HNO_2 is most likely responsible for the catalytic impact on dissolution rate.[3] A solution containing 8 M HNO_3 at 100 ˚C was selected for the dissolutions.

Initially, the sparge gas flowrate was set at 12 cm^3/min, but the flowrate was not sufficient to overcome the liquid head from the solution in the sparger line. In Experiment 134, a NO flowrate of 50 cm^3/min was used to overcome the liquid head in the sparger line and provide a large amount of bubbles below the coupon basket. In Experiment 135, a NO flowrate of 35 cm^3/min was used to reduce the amount of bubbles below the coupon basket. Table 3-14 and Table 3-15 show the masses and dimensions of the U metal samples as a function of time in Experiment 134 using 8 M HNO_3 at 100 ˚C with a 50 cm^3/min NO sparge and Experiment 135 using 8 M HNO_3 at 100 ˚C with a 35 cm^3/min NO sparge, respectively.

Plots of the mass-to-surface area ratio versus dissolution time for Experiments 129, 134, and 135 are shown in Figure 3-5. The measured dissolution rate is obtained as the slope of a linear regression of the mass-to-surface area ratio versus time. The initial and last point(s) are generally not used in the regression due to the initial induction period and the tailing-off period toward the end of the dissolutions. Based on the linear regressions, the dissolution rates for the U metal sample at the various NO sparge rates are shown in Table 3-16. The data show that in Experiment 134 with a NO sparge rate of 50 cm^3/min, the dissolution rate increased about 50% compared to the dissolution rate when the solution was not sparged with NO (Experiment 129). However, in Experiment 135 with a lower NO sparge rate of 35 cm^3/min, the dissolution rate increased about 300% when compared to the dissolution rate of the unsparged solution. Based on visual observation (Figure 3-6), the use of a 50 cm^3/min NO sparge produced a large amount of bubbles around the U metal sample resulting in a mass transfer limitation which interfered with the HNO_3/HNO_2 reactions at the surface of the metal. The lower NO sparge rate was sufficient to promote the generation of HNO_2,

but not high enough to interfere with the dissolution of the U metal. The use of NO gas to catalyze U metal dissolution is a viable option and is recommend for applications where high purity $UO_2(NO_3)_2$ is required. For comparison, the dissolution rate measured using 8 M HNO_3 at 100 ˚C with a 35 cm^3/min NO sparge was about the same as the dissolution rate measured using 10 M HNO_3 at boiling (114 ˚C). A disadvantage of using NO gas to catalyze U metal dissolution is the increased offgas handling requirements.

Table 3-14. Exp 134 – U Metal Dissolution Rate Data for 8 M HNO_3 at 100 ˚C using a 50 cm^3/min NO Sparge

Time (min)	Mass (g)	Diameter (mm)	Length (mm)	Surface Area (SA) (cm^2)	Mass/SA (mg/cm^2)
0.0	3.4875	2.87	29.73	2.810	1241.12
16.4	3.2259	2.80	29.34	2.704	1193.00
31.7	2.2646	2.54	28.66	2.388	948.20
38.4	1.8754	2.44	28.62	2.287	819.89
49.0	1.3787	1.9	28.21	1.741	792.10
56.2	1.1014	1.81	28.12	1.650	667.34
64.6	0.8245	1.61	27.90	1.452	567.88
75.5	0.5337	1.42	27.72	1.268	420.81
86.8	0.2965	0.99	27.17	0.860	344.59
124.4	0	0	0	0	0

Table 3-15. Exp 135 – U Metal Dissolution Rate Data for 8 M HNO_3 at 100 ˚C using a 35 cm^3/min NO sparge

Time (min)	Mass (g)	Diameter (mm)	Length (mm)	Surface Area (SA) (cm^2)	Mass/SA (mg/cm^2)
0.0	2.86	38.66	0.0	3.602	907.01
15.2	2.86	39.22	15.2	3.652	750.47
25.1	2.55	39.23	25.1	3.245	489.66
35.3	2.24	35.5	35.3	2.577	244.00
58.0	0	0	58.0	0	0

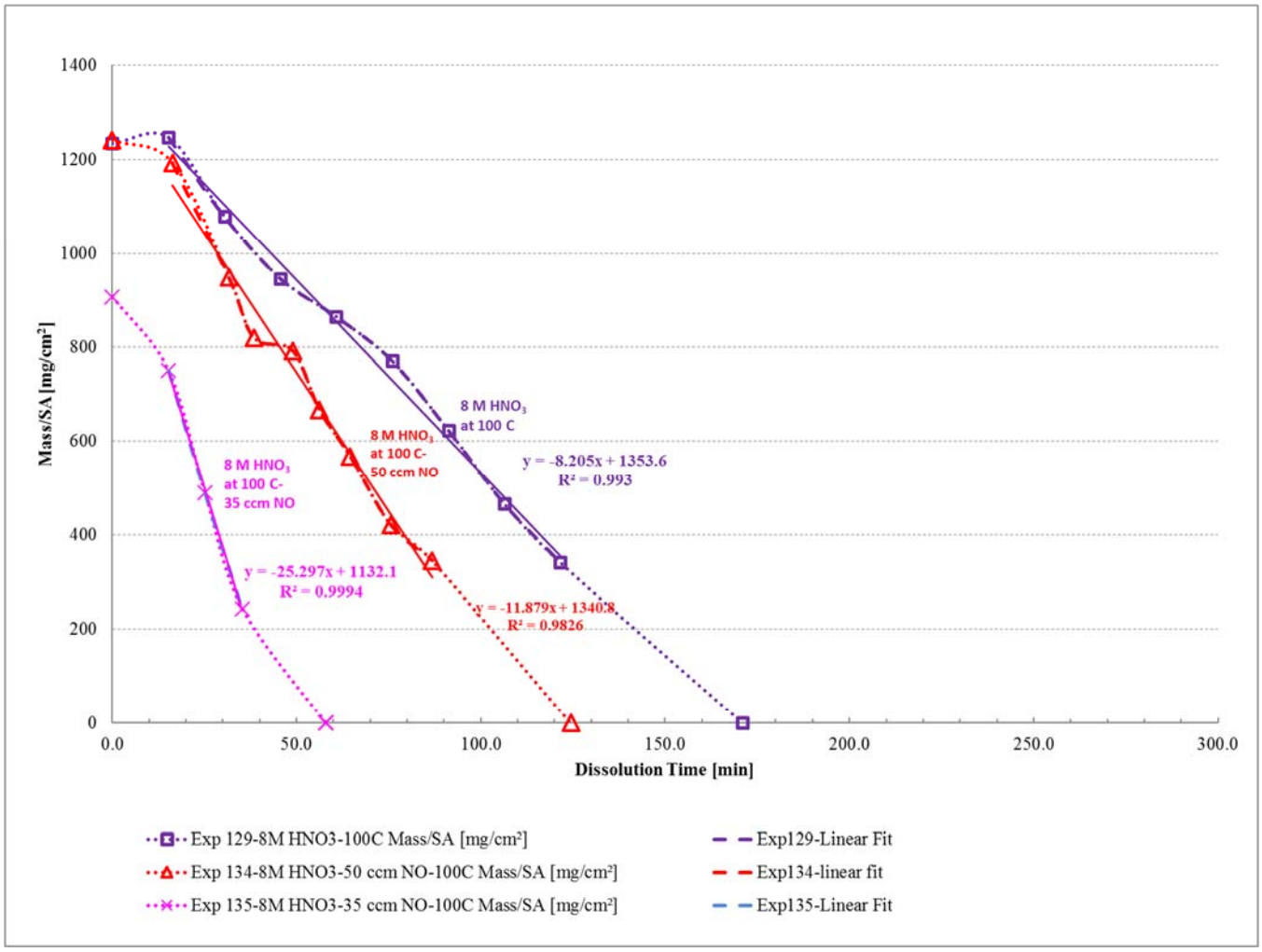

Figure 3-5. Calculation of U Metal Dissolution Rate as a Function of the NO Sparge Rate

Table 3-16. U Metal Dissolution Rates at 8 M HNO_3 as Function of the NO Sparge Rate

Exp. No.	Dissolution Temperature	Dissolution Rate	NO Sparge Rate
---	(˚C)	($mg/cm^2/min$)	(cm^3/min)
129	100	8.2	0
134	100	11.9	50
135	100	25.3	35

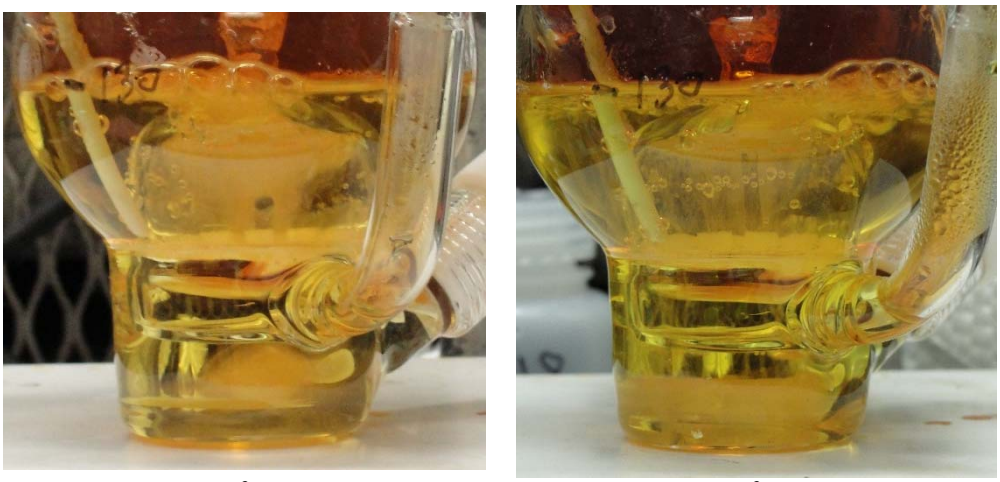

Exp 134 – 50 cm^3/min NO Sparge **Exp 135 – 35 cm^3/min NO Sparge**

Figure 3-6. NO Bubbling Rate during U Metal Dissolution

3.2 Flammable Gas Generation

The generation of flammable gas (i.e., H_2) during the dissolution of nuclear materials is an issue which must be addressed. The concentration of H_2 in the offgas from a dissolution must be controlled below the lower flammability limit. The offgas generation rate during the dissolution of U metal and the characterization of its composition were investigated by Daniel et al.[11] In the prior work, the authors showed that the offgas generation rate was low and the concentration of H_2 was inconsequential. For these reasons, no additional offgas studies were performed as a part of this task. The generation of flammable gas during the dissolution of U metal for the fabrication of UO_2 targets for ^{99}Mo production is not an issue.

4.0 Conclusions and Recommendations

Uranium metal dissolution experiments were completed to measure the effects of HNO_3 concentration, temperature, and the catalytic effects of fluoride and NO gas on the rate of dissolution. A series of experiments with increasing HNO_3 concentration demonstrated that the dissolution rate was a strong function of the acid concentration consistent with data in the literature. The dissolution rate increased by a factor of 12 between 4 and 10 M HNO_3. The optimum HNO_3 concentration for a U metal dissolution process depends upon the desired cycle time and the acid concentration required for downstream processing. Uranium metal dissolutions are not a strong function of temperature relative to acid strength. An increase in temperature from 90 to 110 ˚C during dissolutions performed in 8 M HNO_3 only resulted in a doubling of the rate. However, unless there is a reason to use a temperature less than the boiling point of the solution (e.g., safety concerns), performing U metal dissolutions at the boiling point is recommended to maximize the dissolution rate.

The use of fluoride and NO gas to catalyze U metal dissolution was evaluated in separate series of experiments. For the addition of fluoride to have a significant effect on the U metal dissolution rate, concentrations greater than 0.01 M were required. When 0.01 M fluoride was added to the dissolving solution, there was not a significant change in the dissolution rate from an experiment performed with no fluoride in the solution. When 0.05 and 0.10 M fluoride were added to the solution, the measured rates increased by factors of approximately two and eight, respectively. The ineffectiveness of 0.01 M fluoride in catalyzing the U metal dissolution is likely due to the complexation of the fluoride by the U in solution. The use of fluoride to catalyze U metal dissolution must be balanced against the potential for corrosion of downstream equipment and the addition of corrosion products to the U stream. Although, fluoride is soluble in the ADU precipitation process proposed to isolate the U, decontamination factors for soluble species

during precipitations are generally low without significant washing of the precipitate which adds to the waste volume.

The use of NO gas to catalyze U metal dissolution is a viable option to accelerate the dissolution rate. Its use is recommended for applications where high purity $UO_2(NO_3)_2$ is required. In the laboratory experiments, U metal dissolved using an 8 M HNO_3 solution at 100 ˚C while sparging with 35 cm^3/min of NO gas resulted in about a threefold increase in the dissolution rate compared to the experiment performed with no sparging under the same conditions. The dissolution rate was approximately equal to the rate measured when 10 M HNO_3 at boiling (114 ˚C) was used to dissolve U metal. The effectiveness of NO gas as a catalyst is dependent on the flowrate and the dissolver and sparger design. The flowrate of NO should be selected based on the dissolver volume and the sparger designed to saturate the solution with NO. The NO sparge should not impinge directly upon the U metal which would result in a mass transfer limitation which interferes with HNO_3/HNO_2 reactions at the surface of the metal. A disadvantage of using NO gas to catalyze U metal dissolution is the increased offgas handling requirements.

5.0 References

1. Nuclear Science Advisory Committee ^{99}Mo Subcommittee, *Annual Assessment of the NNSA-Material Management and Minimization (M^3) ^{99}Mo Program*, US Department of Energy Office of Science, Washington, DC (March 19, 2018).
2. R. P. Larsen, *Dissolution of Uranium Metal and Its Alloys*, Anal Chem, Vol. 31, No. 4, p. 545-549 (1959).
3. J. R. Lacher, J. D. Salzman, J. D. Park, *Dissolving Uranium in Nitric Acid*, Ind Eng Chem, Vol.53, No. 4, p. 282-284 (1961).
4. S. M. Stoller and R. B. Richards, Eds., *Reactor Handbook, Volume II, Fuel Reprocessing*, p. 60-61, Interscience Publishers, Inc., New York, NY (1961)
5. T. J. Colven, C. W. Cline, and A. E. Wible, *Processing of Irradiated Natural Uranium at Savannah River*, DP-500, E I. du Pont de Nemours & Co., Aiken, SC (August 1960).
6. T. F. Evans, *Pilot Plant Dissolution of Unjacketed Fuel Elements*, HW-46093, General Electric Company, Richland, WA (1956).
7. W. C. Perkins and R. M. Wallace, *Plant Problems During Dissolution of Uranium Metal Scrap*, DPST-77-204, E. I. du Pont de Nemours & Co., Aiken, SC (January 10, 1977).
8. F. A. Cotton and G. Wilkinson, *Advanced Inorganic Chemistry*, 5th ed., John Wiley & Sons, New York, NY, p. 324-327 (1988).
9. R. L. Moore, W. W. Schulz, and S. J. Walter, *Phosphate Catalysis in Nitric Acid Dissolution of Uranium Metal*, HW-28995, General Electric Company, Richland, WA (July 31, 1953).
10. R. A. Pierce, *Uranium Metal Dissolution in the Presence of Fluoride and Boron*, WSRC-TR-2003-00500, Westinghouse Savannah River Company, Aiken, SC (November 2003).
11. W. E. Daniel, T. S. Rudisill, P. M. Almond, and P. E. O'Rourke, *Dissolution of Low Enriched Uranium from the Experimental Breeder Reactor-II Fuel Stored at the Idaho National Laboratory*, SRNL-STI-2017-00263, Savannah River National Laboratory, Aiken, SC (June 2017).
12. M. F. Simpson, *Developments of Spent Nuclear Fuel Pyroprocessing Technology at Idaho National Laboratory*, INL-EXT-12-25124, Idaho National Laboratory, Idaho Falls, ID (March 2012).
13. M. N. Patterson, *Recovered LEU to Savannah River H-Canyon*, Idaho National Laboratory, Idaho Falls, ID (May 20, 2015).
14. R. R. Hamer, *A Determination of the Stability Constants of a Number of Metal Fluoride Complexes and Their Rates of Formation*, ENICO-1004, Exxon Nuclear Idaho Company, Inc., Idaho Falls, ID (August 1979).

15. E. A. Kyser, *Decontamination of Plutonium from Fluoride and Chloride during Oxalate Precipitation, Filtration and Calcination Processes*, SRNL-SRI-2012-00443, Savannah River National Laboratory, Aiken, SC (July 2012)

Distribution:

T. B. Brown, 773-A
A. D. Cozzi, 999-W
D. A. Crowley, 773-43A
D. E. Dooley, 773-A
A. P. Fellinger. 773-42A
S. D. Fink, 773-A
N. V. Halverson, 773-42A
E. K. Hansen, 999-W
C. C. Herman, 773-A
D. T. Herman, 735-11A
K. M. Fox, 999-W
J. J. Mayer II, 999-W
D. J. McCabe, 773-42A
G. A. Morgan Jr, 999-W
F. M. Pennebaker, 773-42A
W. G. Ramsey, 999-W
L. T. Reid, 773-A
M. E. Stone, 999-W
B. J. Wiedenman, 773-42A
W. R. Wilmarth, 773-A
P. M. Almond, 773-A
N. J. Bridges, 773-A
W. E. Daniel Jr, 999-W
J. M. Duffey, 773-A
H. W. Eldridge, 773-A
N. S. Karay, 773-A
E. A. Kyser III, 773-A
K. P. McCann, 773-A
R. A. Pierce, 773-A
T. S. Rudisill, 773-A
T. C. Shehee, 773-A
T. W. Smith, 773-A
J. E. Klein, 773-A
A. S. Poore, 999-2W
W. H. Clifton Jr, 704-2H

Records Administration (EDWS)